Current Optics and Photonics
Vol. 5, No. 2, April 2021, pp. 129–133

ISSN: 2508-7266(Print) / ISSN: 2508-7274(Online)
DOI: https://doi.org/10.3807/COPP.2021.5.2.129

Performance of an InAs/GaSb Type-II Superlattice Photodiode with Si_3N_4 Surface Passivation

Ha Sul Kim*

Department of Physics, Chonnam National University, Gwangju 61186, Korea

(Received November 27, 2020 : revised January 21, 2021 : accepted January 22, 2021)

This study observed the performance of an InAs/GaSb type-II superlattice photodiode with a *p-i-n* structure for mid-wavelength infrared detection. The 10 ML InAs/10 ML GaSb type-II superlattice photodiode was grown using molecular beam epitaxy. The cutoff wavelength of the manufactured photodiode with Si_3N_4 passivation on the mesa sidewall was determined to be approximately 5.4 and 5.5 μm at 30 K and 77 K, respectively. At a bias of −50 mV, the dark-current density for the Si_3N_4-passivated diode was measured to be 7.9×10^{-5} and 1.1×10^{-4} A/cm^2 at 77 K and 100 K, respectively. The differential resistance-area product R_dA at a bias of −0.15 V was 1481 and 1056 Ω cm^2 at 77 K and 100 K, respectively. The measured detectivity from a blackbody source at 800 K was calculated to be 1.1×10^{10} cm Hz$^{1/2}$/W at zero bias and 77 K.

Keywords : InAs/GaSb, Infrared detector, Passivation, Superlattice
OCIS codes : (040.1880) Detection; (040.3060) Infrared; (040.5160) Photodetectors; (040.5350) Photovoltaic

I. INTRODUCTION

Infrared photodetectors can be used in a variety of applications, from thermal imaging sensors used in the detection of infectious diseases such as COVID-19 to thermal target-tracking sensors used in the military. As an uncooled infrared detector, a microbolometer based on vanadium oxide (VO_x) has been used to detect the long-wavelength infrared (LWIR) spectrum near the 10-μm region [1]. However, a microbolometer has low speed and resolution in temperature measurement. To overcome these inferior properties, cryogenically or thermoelectrically cooled detectors have been used in high-speed and high-precision measurements in mid- and long-wavelength infrared detection. For example, although cooled InSb detectors are commonly used in the mid-wavelength infrared (MWIR) spectral region, this material has a fixed band gap [1]; therefore, changes to the cutoff wavelength in the detector are impossible. By utilizing another material used in LWIR detection, a mercury cadmium telluride (MCT) detector equipped with an expansive cooling unit has been used, owing to its wideband detection of around 9–12 μm. However, the growth of the MCT material in uniform composition at the wafer scale is difficult.

The InAs/GaSb type-II superlattice (T2SL) has been considered as a promising alternative material to replace InSb or MCT materials for infrared detection in thermal imaging. The band gap of an InAs/GaSb T2SL can be adjusted between 3 and 30 μm, according to the thickness of InAs and GaSb. In addition, the carrier lifetime of an InAs/Ga(As)Sb T2SL is expected to be longer than that of MCT for the same cutoff wavelength, owing to the suppression of Auger recombination [2]. In addition, research on the high-quality growth technology of T2SL material has recently achieved rapid progress. Therefore, InAs/GaSb T2SL material is considered to be a strong candidate to replace expensive InSb or MCT materials for infrared detection in the future [3].

Around 15 years ago, 8 monolayer (ML) InAs/8 ML GaSb T2SL devices for mid-wavelength detection were

*Corresponding author: hydenkim@jnu.ac.kr, ORCID 0000-0001-7272-7052
Color versions of one or more of the figures in this paper are available online.

developed by several research groups. Rodriguez *et al*. reported that the nBn structure based on a 8 ML InAs/8 ML GaSb T2SL represented a specific detectivity D^* of approximately 10^9 cm $Hz^{1/2}$/W at 4.5 μm and 300 K [4]. In 2009, Ting *et al*. introduced a complementary barrier infrared detector, showing a D^* of 1.1×10^{11} cm $Hz^{1/2}$/W with a 50% cutoff wavelength of 9.9 μm [5]. In 2012, Salihoglu *et al*. suggested an N-structure T2SL exhibiting a D^* of 2.6×10^{10} at 125 K and a cutoff wavelength of 4.3 μm [6]. Last year, Wu *et al*. demonstrated a high-performance InAs/-InAsSb T2SL mid-wavelength infrared photodetector with a double-barrier structure, which resulted in a D^* of 6.9×10^{11} cm $Hz^{1/2}$/W at 150 K with a cutoff wavelength of 3.9 μm [7]. These diverse architectures of the T2SL structure have provided scientists with a high-performance IR detector operable even at high temperatures.

In this research, we attempted to broaden the cutoff wavelength of the InAs/GaSb T2SL structure by increasing the thicknesses of both InAs and GaSb from 8 ML to 10 ML, thereby narrowing the band gap of the T2SL. Extension of the cutoff wavelength above 5 μm can allow for applications in temperature monitoring from –50 to 250 °C [8]. However, a semiconductor detector with a narrow band gap suffers from increasing noise and dark-current density. To overcome these disadvantages, we attempted device passivation on the mesa sidewall to reduce the leakage current and increase the signal-to-noise ratio.

Several research groups have conducted passivation studies of the InAs/GaSb T2SL photodetector by using dielectric films such as Al_2O_3 or SiO_2, and have demonstrated reduction of dark-current density by one or two orders of magnitude. Salihoglu *et al*. [9] used Al_2O_3 as a passivation material on a mid-wavelength InAs/GaSb T2SL. The results showed a dark-current density reduced by approximately one order of magnitude compared to that of an unpassivated photodiode, owing to advantageous Gibbs free energy and self-healing during the atomic layer deposition process of Al_2O_3 [9]. As another example, Herrera *et al*. [10] passivated the sidewall of InAs/GaSb T2SL photodiodes with SiO_2 films. They analyzed various effects of the passivation layers and observed the formation of As clusters between the T2SL and SiO_2 layer. The dark-current density of a photodiode passivated with a SiO_2 layer decreased by more than one order of magnitude, compared to that of an unpassivated T2SL photodiode.

Recently, the dynamic resistance-area product of an InAs/GaSb T2SL device passivated with Si_3N_4 at zero bias was shown to be higher than that of a device passivated with SiO_2 at temperatures ranging to 100 K, owing to the relatively low thermal stress between GaSb and Si_3N_4 [11]. This means that Si_3N_4 film may be a better passivation material than SiO_2 film, under certain temperature regions and growth conditions of the Si_3N_4 film. Therefore, we used Si_3N_4 as the passivation layer in this study, and evaluated the electrical and optical characteristics of a 10 ML InAs/10 ML GaSb T2SL photodiode with a *p*-*i*-*n* structure.

II. EXPERIMENTS AND DISCUSSION

After loading the GaSb substrate into the molecular beam epitaxy (MBE) system, the wafer substrate was heated to remove the naturally generated gallium oxide thin film. A sacrificial layer of GaSb was grown on the top surface of the substrate, and an In (As, Sb) lattice matched to the GaSb substrate was grown at approximately 200 nm. For the T2SL growth of the *p*-*i*-*n* structure, 80 cycles of 10 ML InAs ($n = 2 \times 10^{18}$ cm^{-3})/10 ML GaSb were grown as a common bottom-contact layer. 300 cycles of 10 ML InAs/10 ML GaSb (Be, $p = 1 \times 10^{15}$ cm^{-3}) were grown to serve as the infrared-absorbing layer. Finally, GaSb ($p = 2 \times 10^{18}$ cm^{-3}) was grown at approximately 200 nm as a top-contact semiconductor.

The grown wafer was subjected to structural analysis using an x-ray diffractometer (XRD) to determine the growth structure, and then we fabricated the InAs/GaSb T2SL photodiode using a conventional semiconductor process. In the beginning, a positive photoresist was applied using spin coating. After exposure and development, the positive photoresist of the mesa-definition structure was left on top of the grown wafer. Thereafter, etching was performed on the bottom contact layer with an inductively-coupled-plasma etching system using BCl_3 gas. Then Si_3N_4 was deposited using plasma-enhanced chemical vapor deposition; at this time, the temperature inside the chamber was maintained at 300 °C, and the final deposition thickness of the Si_3N_4 film was fixed at 200 nm. Next the Si_3N_4 film was removed through dry etching, excluding the mesa sidewall. Finally, Ti-Au was simultaneously deposited onto the *p*-type GaSb and *n*-type T2SL layers using an electron-beam evaporator as an Ohmic metal contact material. The manufactured InAs/GaSb T2SL was mounted onto a lead-free chip carrier using melted indium by heating it to 160 °C on a hotplate. Wire bonding with Au was performed to evaluate the electrical and optical properties of the device. Figure 1 presents the structural schematic diagram of the photodetector structure.

Figure 2 shows a spectral-response measurement system comprising a Fourier-transform infrared spectroscope (FTIR), cryostat, current amplifier, detector interface unit, and computer with the commercial software Omnic for spectrum acquisition. The fabricated device was mounted onto a cold finger in the helium closed-cycle cryostat. The temperature of the InAs/GaSb T2SL device was adjusted by a heater in the cryostat via an external electric power source, in agreement with the setup temperature. The spectral response from 2.5 to 6 μm was measured using the FTIR and analyzed using Omnic.

Figure 3 shows the spectra observed at device temperatures of 30 K and 77 K. The cutoff wavelength of the device was observed to be 5.4 μm and 5.5 μm at 30 K and 77 K, respectively. As the temperature of the photodiode increased, a shift in cutoff wavelength of 0.1 μm was observed, owing to the band-gap shrinkage of the T2SL

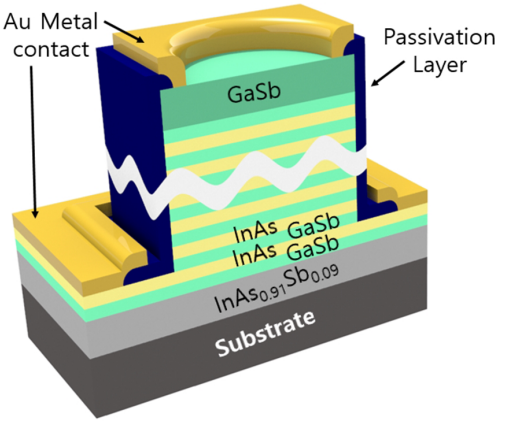

FIG. 1. Schematic diagram of the 10 ML InAs/10 ML GaSb type-II superlattice photodetector with *p-i-n* structure.

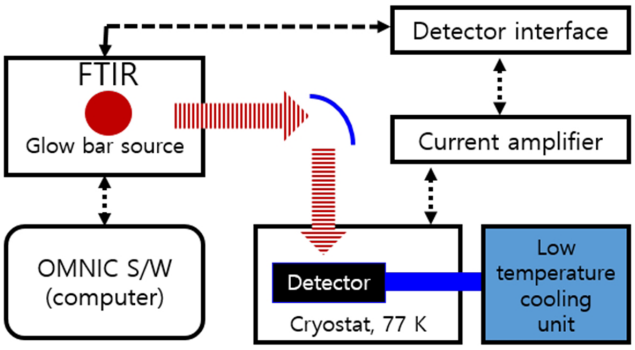

FIG. 2. Spectral-response measurement system, comprising a Fourier transform infrared spectroscope (FTIR), cryostat, and current amplifier for spectrum acquisition.

device. The intensity of the spectrum decreased by approximately 10% at 3 μm, compared to the maximum peak intensity at 30 K; on the other hand, the intensity of the spectrum decreased by approximately 30% at 3 μm, compared to the maximum peak intensity at 77 K. It is believed that the wave-function overlap of InAs/GaSb T2SL at 77 K decreased compared to that at 30 K, owing to the strain valence difference depending on the temperature. In addition, the absorption peak of the spectral response in the 4.3 μm band was observed in both cases at 30 K and 77 K, owing to the infrared light absorption by CO_2 gas, which was in the atmosphere between the detector and glow-bar light source in the FTIR. There was no change in the difference in spectral intensity as a function of the applied bias.

The dark current of the InAs/GaSb T2SL photodiode was measured over a temperature range of 50 to 300 K using a semiconductor parameter analyzer, which was connected to the cryostat shown in Fig. 2. The photodiode was covered by a special cylindrical cover in the helium closed-cycle cryostat, so that the infrared rays emitted from the room-temperature background radiation in the laboratory were blocked during the dark-current measurement. Figure 4 shows the results for the current density of the InAs/GaSb

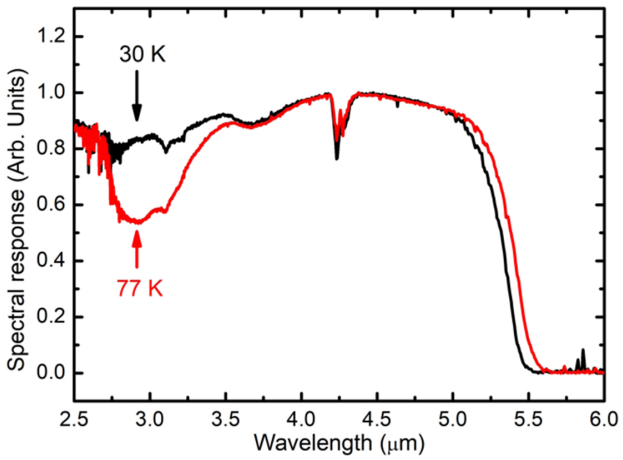

FIG. 3. Observed spectrum of the InAs/GaSb T2SL photodiode using the spectral-response measurement system, at 30 K and 77 K.

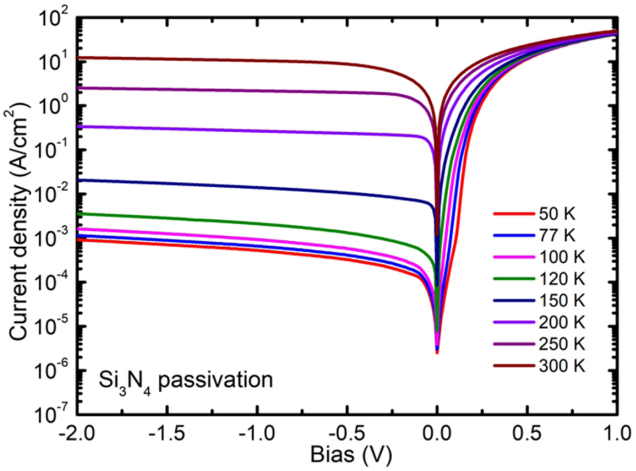

FIG. 4. Current density of the InAs/GaSb T2SL device with Si_3N_4 passivation, for applied bias ranging from −2.0 to 1.0 V.

T2SL device with Si_3N_4 passivation, for applied bias ranging from −2.0 to 1.0 V. The measured dark-current density under a bias of −50 mV was 7.9×10^{-5} and 1.1×10^{-4} A/cm^2 at 77 K and 100 K, respectively.

Figure 5 presents dark-current densities as a function of temperature at a bias of −50 mV. For temperatures greater than 120 K, the dark-current density of the diode shows diffusion-limited behavior. In contrast, for temperatures less than 120 K the dark-current density of the diode exhibits saturated behavior, which is related to generation-recombination and other dark-current sources, such as trap assistance, surface tunneling, or shortage of device passivation. We are currently conducting device simulations of this electrical behavior, and the results will be reported in the future. Figure 6 presents the differential resistance-area product R_dA as a function of temperature for the T2SL photodiode at a bias of −0.15 V. The calculated R_dA was about 1481 Ω cm^2 at 77 K and about 1056 Ω cm^2 at 100 K. Martyniuk *et*

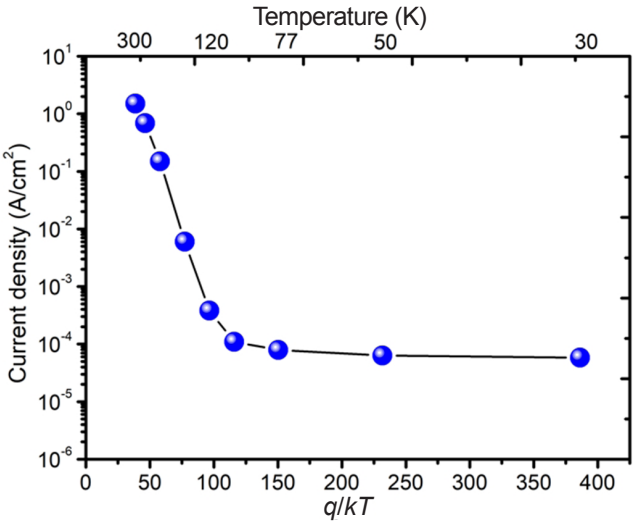

FIG. 5. Dark-current density as a function of temperature, at a bias of −50 mV.

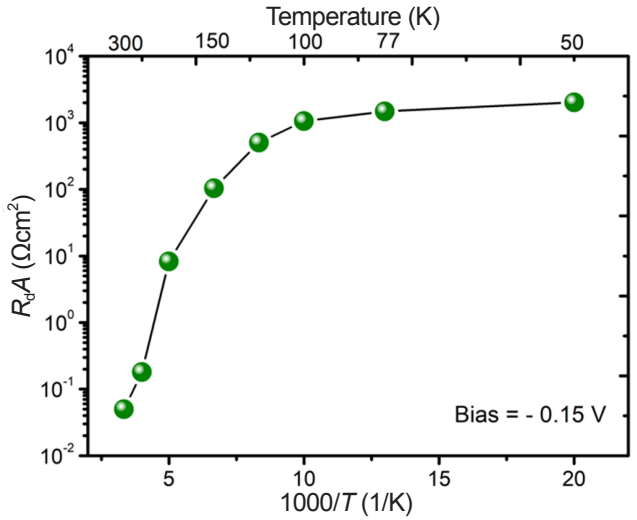

FIG. 6. Differential resistance-area product R_dA as a function of the temperature of the T2SL photodiode, at a bias of −0.15 V.

al. [12] reported modeling of a mid-wavelength infrared 10 ML InAs/10 ML GaSb type-II superlattice detector with nBn structure, exhibiting a R_dA of 1000 Ω cm^2 at zero bias and 77 K. Therefore, the fabricated detector presented an improvement of approximately 48% in magnitude of RA, compared to the result of Marttniuk *et al*. [12].

Figure 7 presents a block diagram of the measurement system used to acquire the signal and noise values presented in this report. We used a calibrated blackbody source (800 K), a fast Fourier transform (FFT) network signal analyzer (SR 770), an optical chopper (400 Hz), a preamplifier (Keithley 428) and a liquid-nitrogen-cooled dewar. To measure the detectivity (D*, in cm Hz$^{1/2}$/W) of the device using a blackbody source, we calculated the spectral voltage responsivity using the following equation [13]:

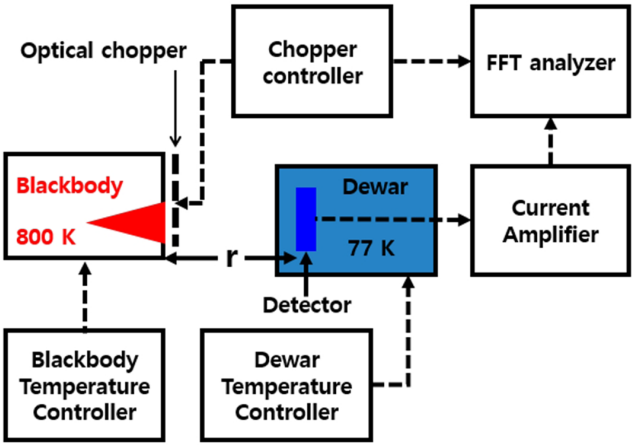

FIG. 7. Block diagram of the measurement system used to acquire the signal and noise values for the InAs/GaSb T2SL photodiode.

$$R(\lambda_c, f) = \frac{v_0}{\left[\frac{hc}{\lambda_c}\right]\left[\frac{A_s A_d}{\pi r^2} t F_F\right]\left[\int_0^{\lambda_c} \frac{2c\pi}{\lambda^4 (exp\{hc/k\lambda T\} - 1)} d\lambda\right]}, \quad (1)$$

where v_0 is the output voltage produced by the detector, h is Planck's constant, c is the speed of light, λ_c is the cutoff wavelength of the detector, A_s is the blackbody area, A_d is the optically active detector area, t is the transmittance, F_F is the form-factor conversion, r is the distance from source to detector, k is Boltzmann's constant, T is the temperature, and λ is the wavelength. A modulated infrared source from a blackbody was used instead of constant blackbody irradiance. The signal amplitude of the sinusoidal infrared input was measured by considering the modulation factor of the mechanical chopper and the opening area of the blackbody source, to reduce calculation error for the responsivity.

The terms in the denominator of Eq. (1) represent the photon energy at peak wavelength, geometrical configurations of the blackbody and detector, and photon exitance integrated over the open detector area. D* was calculated using the following equation [14]:

$$D^* = \frac{R\sqrt{A_d}}{N/\sqrt{\Delta f}}, \quad (2)$$

where R is the responsivity, A_d is the detector area, N is noise, and Δf is the noise-equivalent electrical bandwidth. The noise spectrum from the photodetector was measured using an SR770 network analyzer, which was connected to the detector through a low-noise preamplifier (Keithley 428). Martyniuk *et al*. [12] published their measured D* of 4×10^9 cm Hz$^{1/2}$/W at 240 K and 50 mV bias, for a 10 ML InAs/10 ML GaSb T2SL detector. Figure 8 presents our calculated D* under applied bias using Eqs. (1) and (2). In this study, the calculated D* value was 1.1×10^{10} cm Hz$^{1/2}$/W at 77 K under zero bias. D* rapidly decreased, due to the increased noise current under high positive or negative bias.

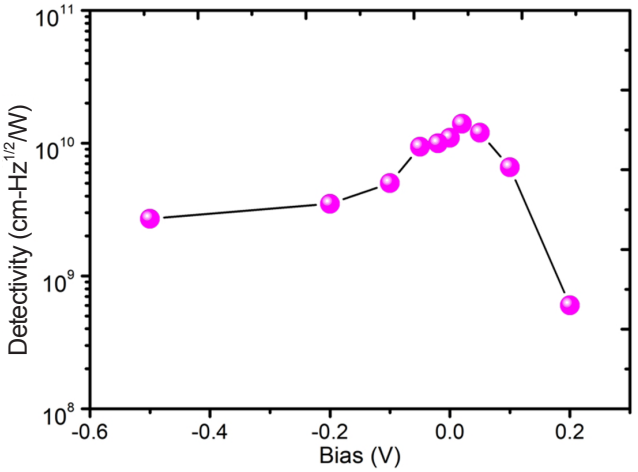

FIG. 8. Calculated detectivity using a blackbody source, at applied bias from −0.5 to +0.2 V at 77 K.

III. CONCLUSION

The performance of a 10 ML InAs/10 ML GaSb T2SL photodiode with a *p-i-n* structure was measured for MWIR detector applications. The T2SL structure was grown with an MBE system, and device fabrication was conducted by a conventional semiconductor-fabrication procedure. To reduce the dark current, we applied Si_3N_4 passivation on the mesa sidewalls using plasma-enhanced chemical vapor deposition. The measured cutoff wavelengths of the T2SL photodiode using FTIR were approximately 5.4 μm at 30 K and 5.5 μm at 77 K. Therefore, the cutoff wavelength for the 10 ML InAs/10 ML GaSb T2SL was approximately 1 μm longer than that for an 8 ML InAs/ 8 ML GaSb T2SL, owing to the shrinking band gap of T2SL at 77 K. The dark-current density of the Si_3N_4-passivated diode under a bias of −50 mV was measured to be 7.9×10^{-5} and 1.1×10^{-4} A/cm^2 at 77 K and 100 K, respectively. The differential resistance-area product R_dA at a bias of −0.15 V was 1481 and 1056 Ω cm^2 at 77 and 100 K, respectively. The detectivity of the 10 ML InAs/10 ML GaSb T2SL photodiode using a blackbody source at 800 K was calculated as 1.1×10^{10} cm Hz$^{1/2}$/W at zero bias and 77 K. Therefore, the 10 ML InAs/10 ML GaSb T2SL may be a promising photodetector material in the MWIR region of approximately 5 μm in the near future.

ACKNOWLEDGMENT

This study was supported by a grant from the Basic Science Research Program through the National Research Foundation of Korea (NRF) funded by the Ministry of Science, ICT and Future Planning (2017R1A2B4007390). In addition, Hun Lee helped with the measurements conducted in this study.

REFERENCES

1. A. Rogalki, "Next decade in infrared detectors," Proc. SPIE **10433**, 104330L (2017).
2. B. V. Olson, C. H. Grein, J. K. Kim, E. A. Kadlec, J. F. Klem, S. D. Hawkins, and E. A. Shaner, "Auger recombination in long-wave infrared InAs/InAsSb type-II superlattices," Appl. Phys. Lett. **107**, 261104 (2015).
3. A. Rogalski, P. Martyniuk, and M. Kopytko, "InAs/GaSb type-II superlattice infrared detectors: Future prospect," Appl. Phys. Rev. **4**, 031304 (2017).
4. J. B. Rodriguez, E. Plis, G. Bishop, Y. D. Sharma, H. Kim, L. R. Dawson, and S. Krishna, "*nBn* structure based on InAs/GaSb type-II strained layer superlattices," Appl. Phys. Lett. **91**, 043514 (2007).
5. D. Z.-Y. Ting, C. J. Hill, A. Soibel, S. A. Keo, J. M. Mumolo, J. Nguyen, and S. D. Gunapala, "A high-performance long wavelength superlattice complementary barrier infrared detector," Appl. Phys. Lett. **95**, 023508 (2009).
6. O. Salihoglu, A. Muti, K. Kutluer, T. Tansel, R. Turan, Y. Ergun, and A. Aydinli, "'N'structure for type-II superlattice photodetectors," Appl. Phys. Lett. **101**, 073505 (2012).
7. D. Wu, J. Li, A. Dehzangi, and M. Razeghi, "High performance InAs/InAsSb type-II superlattice mid-wavelength infrared photodetectors with double barrier," Infrared Phys. Technol. **109**, 103439 (2020).
8. J. Dixon, "Radiation thermometry," J. Phys. E: Sci. Instrum. **21**, 425–436 (1988).
9. O. Salihoglu, Abdullah Muti, and Atilla Aydinli, "A comparative passivation study for InAs/GaSb pin superlattice photodetectors," IEEE J. Quantum Electron. **49**, 661–666 (2013).
10. M. Herrera, M. Chi, M. Bonds, N. D. Browning, J. N. Woolman, R. E. Kvaas, S. F. Harris, D. R. Rhiger, and C. J. Hill, "Atomic scale analysis of the effect of the SiO2 passivation treatment on InAs/GaSb superlattice mesa sidewall," Appl. Phys. Lett. **93**, 093106 (2008).
11. H. S. Kim, "Passivation study of InAs/GaSb type-II strained layer superlattice in mid-wave Infrared photodetector," J. Korean Phys. Soc. **77**, 714–718 (2020).
12. P. Martyniuk, J. Wróbel, E. Plis, P. Madejczyk, W. Gawron, and A. Kowalewski, "Modeling of midwavelength infrared InAs/GaSb type II superlattice detectors," Opt. Eng. **52**, 061307 (2013).
13. E. L. Dereniak and G. D. Boreman, *Infrared Detectors and Systems* (John Wiley & Sons, Hoboken, NJ. USA, 1996), Chapter 6.
14. J. D. Vincent, S. Hodges, J. Vampola, M. Stegall and G. Pierce, *Fundamentals of Infrared and Visible Detector Operation and Testing, 2nd ed.*, (John Wiley & Sons, Hoboken, NJ, USA. 2015), Chapter 1.